

# MODEL OF FLIGHT TECHNICAL ERROR IN SYMMETRICAL PLANE FOR PERFORMANCE BASED NAVIGATION

Zhao Hongsheng<sup>1</sup>, Xu Xiaohao<sup>2</sup>, Zhang Jun<sup>1</sup>, Zhu Yanbo<sup>1</sup>, Yang Chuansen<sup>3</sup>

(1. School of Electronic Information Engineering, Beijing University of Aeronautics and Astronautics, Beijing, 100191, P. R. China; 2. College of Air Traffic Management, Civil Aviation University of China, Tianjin, 300300, P. R. China; 3. College of Civil Aviation, NUAU, 29 Yudao Street, Nanjing, 210016, P. R. China)

**Abstract:** In the performance based navigation (PBN), the flight technical error (FTE) and the navigation system error (NSE) are two main parts of total system error (TSE). The implementation of PBN requires pre-flight prediction and en-route short-term dynamical prediction of TSE. Once the sum of predicted FTE and NSE is greater than the specified PBN value, PBN cannot operate. Thus, it requires accurate modeling and thorough analysis of the two main contributors. Multiple-input multiple-output (MIMO) longitudinal flight control system of ARIC model is designed using the linear quadratic Gaussian and loop transfer recovery (LQG/LTR) method, and FTE in symmetrical plane of aircraft is analyzed during the turbulence disturbed approach. The error estimation mapping function of FTE in symmetrical plane and its bound estimation model are proposed based on the singular value theory. The model provides an approach based on the forming mechanism of FTE, rather than the costly flight test and the data fitting. Real-data based simulation validates the theoretical analysis of FTE in symmetrical plane. It also shows that FTE is partially caused by the turbulence fluctuation disturbance when the automatic flight control system (AFCS) is engaged and increases with escalating the environmental turbulence intensity.

**Key words:** flight technical error; performance based navigation; LQG/LTR; air traffic management; Kalman filter

**CLC number:** V355

**Document code:** A

**Article ID:** 1005-1120(2011)03-0246-09

## INTRODUCTION

The high accuracy and global coverage of global navigation satellite system (GNSS) have enabled it to be the basis of the next generation air traffic management system, in which performance based navigation (PBN) is a fundamental component. Flight technical error (FTE) and navigation system error (NSE) are two components of total system error (TSE) of PBN<sup>[1]</sup>. The safety and efficiency of life-critical flight operation are heavily dependent on the performance of navigation systems, such as accuracy, continuity,

integrity, and availability. But in the generalized sense of PBN, it also requires the satisfying performance of automatic flight control system (AFCS) and pilot. FTE is the limitation of AFCS or human-machine closed-loop manual control system to track desired flight path, maintain intended altitude as well as target velocity with infinite accuracy.

A mixed probability model of vertical FTE during approach was presented in Ref. [2]. The auto-correlation, cross-correlation of vertical and longitudinal FTE were discussed in Ref. [3]. In Ref. [4], vertical FTE of approach segment was

---

**Foundation items:** Supported by the National Basic Research Program of China ("973" Program)(2010CB731805); the Foundation for Innovative Research Groups of the National Natural Science Foundation of China (60921001); the National Key Technologies R&D Program of China(2011BAH24B02); the Basic Scientific Research Foundation of Central Institutions of Higher Education (ZXH2009D006).

**Received date:** 2010-09-02; **revision received date:** 2011-03-08

**E-mail:** zhao-zhengbo@sina.com

measured with position sensors such as the surface detection equipment, the surface measurement radar, etc., and statistical fitting was performed. FTEs in simulation and flight tests for small aircraft transportation system-high volume operation (SATS-HVO) of non-radar and non-tower airports were measured and fitted using probability models in Ref. [5]. A statistical estimation model of lateral FTE according to the definition in PBN was proposed for nominal AFCS model in Ref. [6].

The previous literature focused on the field measurement of FTE during approach or the statistical fitting to measured data. However, the successful implementation of PBN requires pre-flight prediction and en-route short-term prediction of FTE, thus its accurate modeling and thorough analysis are indispensable. This paper proposes the design of longitudinal flight control system, and discusses the turbulence fluctuation model.

## 1 SYSTEM DESIGN USING LQG/LTR METHOD

### 1.1 LQG/LTR method

The prominent linear quadratic Gaussian and loop transfer recovery (LQG/LTR) theory, originally proposed by Doyle and Stein, is a multiple-input multiple-output (MIMO) design method based on optimal control theory. It provides guaranteed stability robustness and keeps performance robustness compared with that of state feedback control by the two step loop-shaping design procedure.

The plant model in state-space form is shown in Eqs. (1,2), where  $\mathbf{w}$  and  $\mathbf{v}$  are the zero-mean Gaussian stochastic processes.  $\mathbf{W}$  and  $\mathbf{V}$  in Eqs. (3,4) are the corresponding covariance matrices respectively.

$$\dot{\mathbf{x}} = \mathbf{A}\mathbf{x} + \mathbf{B}\mathbf{u} + \Gamma\mathbf{w} \quad (1)$$

$$\mathbf{y} = \mathbf{C}\mathbf{x} + \mathbf{v} \quad (2)$$

$$E\{\mathbf{w}\mathbf{w}^T\} = \mathbf{W} \geq 0 \quad (3)$$

$$E\{\mathbf{v}\mathbf{v}^T\} = \mathbf{V} > 0 \quad (4)$$

In Eq. (5)  $J$  is the linear quadratic performance index that minimizes the weighted energy of state variable vector and control vector, where

$\mathbf{Q}$  and  $\mathbf{R}$  are weighting matrices, and  $\mathbf{M}$  is  $\Gamma^T$ .

$$J = \lim_{T \rightarrow \infty} E \left\{ \int_0^T [(\mathbf{M}\mathbf{x})^T \mathbf{Q} \mathbf{M} \mathbf{x} + \mathbf{u}^T \mathbf{R} \mathbf{u}] dt \right\} \quad (5)$$

$$\mathbf{Q} = \mathbf{Q}^T \geq 0, \quad \mathbf{R} = \mathbf{R}^T > 0 \quad (6)$$

$$\mathbf{u} = -\mathbf{K}_c \mathbf{x} \quad (7)$$

The optimal state-feedback matrix  $\mathbf{K}_c$  is given by

$$\mathbf{K}_c = \mathbf{R}^{-1} \mathbf{B}^T \mathbf{P}_c \quad (8)$$

where  $\mathbf{P}_c$  satisfies the algebraic Riccati equation  $\mathbf{A}^T \mathbf{P}_c + \mathbf{P}_c \mathbf{A} - \mathbf{P}_c \mathbf{B} \mathbf{R}^{-1} \mathbf{B}^T \mathbf{P}_c + \mathbf{M}^T \mathbf{Q} \mathbf{M} = 0$  and  $\mathbf{P}_c = \mathbf{P}_c^T \geq 0$ .

The Kalman filter gain matrix  $\mathbf{K}_f$  is given by

$$\mathbf{K}_f = \mathbf{P}_f \mathbf{C}^T \mathbf{V}^{-1} \quad (10)$$

where  $\mathbf{P}_f$  satisfies another algebraic Riccati equation that is dual to Eq. (9) and  $\mathbf{P}_f = \mathbf{P}_f^T \geq 0$ .

$$\mathbf{P}_f \mathbf{A}^T + \mathbf{A} \mathbf{P}_f - \mathbf{P}_f \mathbf{C}^T \mathbf{V}^{-1} \mathbf{C} \mathbf{P}_f + \Gamma \mathbf{W} \Gamma^T = 0 \quad (11)$$

The matrices  $\mathbf{K}_c$  and  $\mathbf{K}_f$  exist, and the closed-loop system is internally stable, provided that the systems with state-space realizations  $(\mathbf{A}, \mathbf{B}, \mathbf{Q}^{1/2} \mathbf{M})$  and  $(\mathbf{A}, \Gamma \mathbf{W}^{1/2}, \mathbf{C})$  are stabilizable and detectable. Namely, any uncontrollable or unobservable modes are asymptotically stable.

Fig. 1 shows the schematic diagram of the structure of LQG compensator interconnected with plant model.

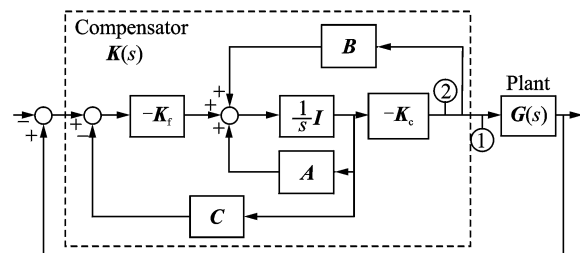


Fig. 1 LQG compensator interconnected with plant model

For the case of designing return ratio at the output of plant, the first step of LQG/LTR is to design a Kalman filter by manipulating the covariance matrices  $\mathbf{W}$  and  $\mathbf{V}$  until a satisfactory return ratio  $-\mathbf{C}(s\mathbf{I} - \mathbf{A})^{-1} \mathbf{K}_f$  is obtained. The second step is to synthesize an optimal state-feedback regulator aiming at recovering the return ratio over a sufficiently large range of frequencies. The regulator is subject to linear quadratic performance index. LTR is achieved by forcing the return ratio at marked point ① in Fig. 1 to approach

that at point ② by tuning weighting matrix. The return ratios at points ① and ② are shown in Eqs. (12,13), respectively.

$$\mathbf{G}(s)\mathbf{K}(s) = -\mathbf{K}_c(s\mathbf{I} - \mathbf{A} + \mathbf{BK}_c + \mathbf{K}_f\mathbf{C})^{-1}\mathbf{K}_f\mathbf{C}(s\mathbf{I} - \mathbf{A})^{-1}\mathbf{B} \quad (12)$$

$$\mathbf{G}(s)\mathbf{K}(s) = -\mathbf{K}_c(s\mathbf{I} - \mathbf{A})^{-1}\mathbf{B} \quad (13)$$

## 1.2 Vertical-plane dynamics model of aircraft

The ARIC model<sup>[7]</sup> is used for analysis giving its comprehensive application as a benchmark.

Hence, for conciseness and the issue focused on primarily, this paper specifies the performance objectives of longitudinal compensated system for ARIC model as follows: There should be zero steady-state error and good damping in the face of step responses or disturbances, with a bandwidth of about 10 rad/s for each loop.

## 1.3 Longitudinal flight controller

The control configuration is firstly presented. Then, the targeted controller is acquired by sequential design of competent Kalman filter and optimal state feedback regulator.

### 1.3.1 Design of control configuration

The dynamics of transport aircraft is linearized during a nominal approach segment to acquire nominal plant data. The air speed is 70.70 m/s, which is the typical velocity for large jets during final approach segment.

With Eqs. (1,2) as the state space model of longitudinal dynamics, the state variable vector, control vector and output vector are chosen as follows

$$\mathbf{x} = [h \quad v \quad \theta \quad q \quad \dot{h}] \quad (14)$$

$$\mathbf{u} = [\delta_s \quad \delta_i \quad \delta_e] \quad (15)$$

$$\mathbf{y} = [h \quad v \quad \theta] \quad (16)$$

where variables in Eq. (14) are the height above ground, the forward speed, the pitch angle, the rate of change of pitch angle, and the vertical speed, sequentially. The variables in Eq. (15) are the spoiler angle, the forward acceleration due to engine thrust and the elevator angle.

Before we proceed to design Kalman filter, the nominal plant is augmented with integrators in both control channels at first to acquire well-damped response. Consequently, three integral

variables are inserted into the state vector

$$\mathbf{x}_a = [h \quad v \quad \theta \quad q \quad \dot{h} \quad \epsilon_s \quad \epsilon_i \quad \epsilon_e] \quad (17)$$

where subscript "a" stands for augmented. To avoid difficulty in the recovery step, we choose a sufficiently small pole of the augmented model in the left hand half plane rather than at origin. The augmentation leads to an increase of 60 dB at 0.001 rad/s for the principal gains of the return ratio  $-\mathbf{C}_a(s\mathbf{I} - \mathbf{A}_a)^{-1}\mathbf{K}_f$ .

### 1.3.2 Design of Kalman filter

The principal gain shaping technique, which is based on the singular value decomposition of  $\mathbf{C}_a(s\mathbf{I} - \mathbf{A}_a)^{-1}\mathbf{\Gamma}\mathbf{W}^{1/2}$  at the frequency to be adjusted, is used to tune open-loop principal gains to obtain 100 dB gain at 0.001 rad/s for  $\underline{\sigma}[-\mathbf{C}_a(s\mathbf{I} - \mathbf{A}_a)^{-1}\mathbf{K}_f]$ , and a band width of 10 rad/s. The latter is equivalent to rendering the cross-over frequency of the compensated system to be  $10/\sqrt{2}$  rad/s.

$$\mathbf{S}_f(s) = [\mathbf{I} + \mathbf{C}_a(s\mathbf{I} - \mathbf{A}_a)^{-1}\mathbf{K}_f]^{-1} \quad (18)$$

$$\mathbf{T}_f(s) = \mathbf{I} - \mathbf{S}_f(s) \quad (19)$$

The control over the principals of the sensitivity function is exercised to acquire the similar behavior of both  $\underline{\sigma}[\mathbf{S}_f(s)]$  and  $\bar{\sigma}[\mathbf{S}_f(s)]$  as they approach 0 dB, with the purpose of reduction in the range of amplified measurement noise and a more homogenous performance in all signal directions. This is achieved at the expense of a larger bandwidth of  $\mathbf{T}_f(s)$ , but with very little increase of  $\|\mathbf{T}_f\|_\infty$  and hence hardly any deterioration of stability margins. Fig. 2 presents the principal gains of both the sensitivity function and the complementary sensitivity function corresponding to the final Kalman filter design.

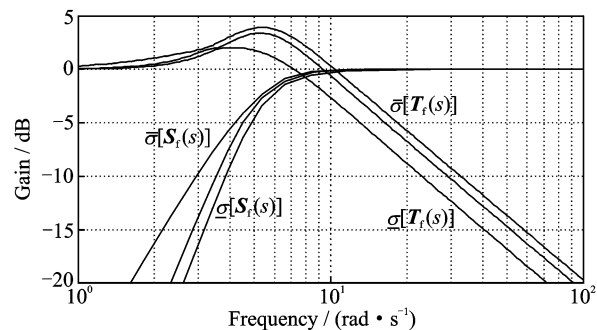


Fig. 2 Principal gains of sensitivity function and complementary sensitivity function

### 1.3.3 LQR design and loop transfer recovery

The optimal state-feedback matrix  $\mathbf{K}_c$  is obtained by solving the Riccati equation (Eq. (9)) with  $\mathbf{M}=\mathbf{C}_a$ ,  $\mathbf{Q}=\mathbf{I}$  and  $\mathbf{R}=\rho\mathbf{I}$ , where  $\rho$  is the parameter to make the return ratio at point ① impend over that at point ② in Fig. 1 as it approaches 0. Eventually, the principal gains of  $\mathbf{G}(s)\mathbf{K}(s)$  are superimposed onto those of  $\mathbf{C}_a(s\mathbf{I} - \mathbf{A}_a)^{-1}\mathbf{K}_f$  for  $\rho=10^{-8}$ , namely adequate recovery is exhibited.

The time domain response of the closed-loop compensated AIRC model is shown in Fig. 3, in which the input commands are height of 277.02 m above ground (touchdown zone), forward speed of 70.7 m/s and a pitch angle of  $3^\circ$  to follow. The response of altitude tracking is reasonably damped and exhibits acceptable maximum overshoot (24.59%) and rise time (0.198 s). It settles within 10% of final value after 0.975 s and reaches final value within 1.5 s. Simultaneously, the maximum overshoot of forward speed is 17.08% and the pitch angle output follows the corresponding reference signal pretty well.

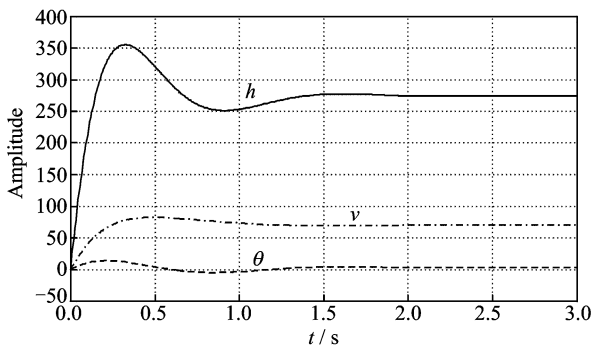


Fig. 3 Time domain response of closed-loop compensated AIRC model

## 2 TURBULENCE FLUCTUATION MODEL

### 2.1 Definition of turbulence model

The Dryden turbulence model based on Taylor's frozen field hypothesis<sup>[8]</sup> is exploited to account for the environmental turbulence disturbance. With the premise that the turbulence fluctuation is stationary, statistically Gaussian distributed with zero mean and homogeneous, the

analytical definition of the power spectra of Dryden model (vertical and longitudinal, shown in Fig. 4) is given as follows

$$\Phi_u(\Omega) = \sigma_u^2 \frac{2L_u}{\pi} \frac{1}{1 + (L_u\Omega)^2} \quad (20)$$

$$\Phi_w(\Omega) = \sigma_w^2 \frac{L_w}{\pi} \frac{1 + 3(L_w\Omega)^2}{[1 + (L_w\Omega)^2]^2} \quad (21)$$

$$\omega = \Omega V \quad (22)$$

where  $u$  and  $w$  are the velocities (ft/s) (1 ft = 0.3078 m) along  $x$ ,  $z$  axes of aircraft respectively ( $x$  axis is along the longitudinal axis of aircraft and nose-direction is positive,  $y$  is orthogonal with symmetrical plane of aircraft and left-wing-direction is positive, positive direction of  $z$  axis is determined with right hand rule),  $\Phi_u$  and  $\Phi_w$  the power spectral densities ( $\text{ft}^3/\text{s}^2$ ) of  $u$ ,  $w$ ,  $\sigma_u$  and  $\sigma_w$  the standard deviations (ft/s) of  $u$ ,  $w$ ,  $L_u$  and  $L_w$  the scale lengths (ft) for power spectra,  $V$  is the air speed of aircraft and  $\Omega$  the spatial frequency. Eq. (23) holds for each of the preceding spectral densities

$$\sigma_{u,w}^2 = \int_0^\infty \Phi_{u,w}(\Omega) d\Omega \quad (23)$$

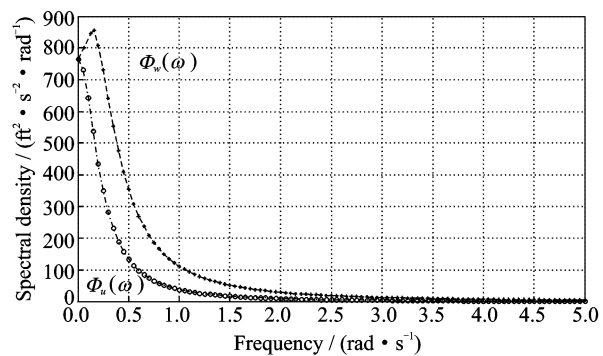


Fig. 4 Power spectral density of vertical and longitudinal Dryden turbulence fluctuation

In Ref. [8], the scale lengths and the standard deviations are specified for two altitude ranges. When the altitude concerned is below 1 000 ft (307.8 m), the values abide by Eqs. (24, 25).

$$\begin{cases} L_w = h \\ L_u = L_v = \frac{h}{(0.177 + 0.000823h)^{1.2}} \end{cases} \quad (24)$$

$$\begin{cases} \sigma_w = 0.1W_{20} \\ \sigma_u = \frac{1}{(0.177 + 0.000823h)^{0.4}} \end{cases} \quad (25)$$

where  $W_{20}$  is the wind speed at 20 ft (6.156 m). For the altitude range above 2 000 ft (615.6 m), the scale lengths are specified as a constant, while the turbulence intensity is a function of altitude as well as probability of exceedance.

## 2.2 Forming filter

The Dryden turbulence<sup>[8]</sup> is generated by adding white Gaussian noise with specified standard deviation into a forming filter for the corresponding direction. The forming filters are shown in Eqs. (26,27), where Eq. (26) is also the forming filter for direction of  $v$  when the subscript is substituted for  $v$ .

$$F_u(s) = \frac{1}{1 + L_u s} \quad (26)$$

$$F_w(s) = \frac{1 + 3^{1/2} L_{ws}}{(1 + L_w s)^2} \quad (27)$$

Eqs. (28,29) prescribe the standard deviation for corresponding axis

$$\sigma_{u_{wn}} = \sigma_u (2L_u/Dx)^{1/2} \quad (28)$$

$$\sigma_{w_{wn}} = \sigma_w (L_w/Dx)^{1/2} \quad (29)$$

where sample step in Descartes frame  $Dx = V \cdot Dt$ , in which  $Dt$  is the sample time-step.  $Dt$  decreases as air speed of aircraft builds up.

## 3 ANALYSIS OF FTE IN SYMMETRICAL PLANE

### 3.1 Propagation of variance

The statistical characteristic of FTE could be described as a normal distribution given FTE is actually a stochastic process<sup>[2]</sup>. This perspective of FTE could be justified by the fact that it is influenced by a number of random variables with various weighting. If we inject the turbulence disturbance signal at input, its statistical characteristics are transmitted to the output through closed-loop system. Thus it will be preferred and beneficial to analyze the propagation of variance with a perspective of the system gain.

### 3.2 Singular value based mapping function

FTE in symmetrical plane (symmetrical plane is defined as the plane including longitudinal axis of aircraft, and orthogonal with the line connecting two wing-tips) consists of the vertical

FTE (FTE of altitude) and the longitudinal FTE (FTE of forward air speed). Thus the altitude and the forward air speeds are two signals considered in output vector. Thus we need to obtain the specific transfer function for each channel from the driven Gaussian noise input. The transfer functions map the environmental turbulence disturbance to  $h$  and  $v$ .

The power spectral density functions of input signal  $u(t)$  and output signal  $y(t)$  are defined as the Fourier transform of their variance as shown in Eqs. (30,31), where  $\tau$  is the time increment.

$$\Phi_{uu}(\omega) = \mathbf{F}[E\{u(t)u(t+\tau)\}] \quad (30)$$

$$\Phi_{yy}(\omega) = \mathbf{F}[E\{y(t)y(t+\tau)\}] \quad (31)$$

On the basis of the foregoing definition, the following formula holds, where  $T(s)$  is the single-input single-output (SISO) transfer function from certain input channel to the interested output signal, and it is acquired from the closed-loop transfer function matrix of the integrated system

$$\Phi_{yy}(\omega) = T(j\omega)\Phi_{uu}(\omega)T(-j\omega) \quad (32)$$

The variance of the individual output signal is obtained with

$$E\{y^2\} = \frac{1}{2\pi} \int_{-\infty}^{\infty} \Phi_{yy}(\omega) d\omega \quad (33)$$

This is indeed the variance of longitudinal FTE or vertical FTE. Thus, we obtain the following equation given that  $T(s)$  is stable.

$$\begin{aligned} E\{y^2\} &= \frac{1}{2\pi} \int_{-\infty}^{\infty} \Phi_{yy}(\omega) d\omega = \\ &= \frac{1}{2\pi} \int_{-\infty}^{\infty} T(j\omega)\Phi_{uu}(\omega)T(-j\omega) d\omega = \\ &= \frac{1}{2\pi} \int_{-\infty}^{\infty} \sigma^2(\Phi_{uu}^{1/2}(\omega)T(j\omega)) d\omega \end{aligned} \quad (34)$$

This mapping function is the basis of the bound estimation model of FTE in symmetrical plane. Note that  $\sigma$  without subscript in Eq. (34) is the maximum amplitude-frequency gain of  $T(s)$ , and can be read from the Bode magnitude plot. In Section 2, the symbol " $\sigma$ " with subscripts is used to denote the turbulence intensity. Note that Bode magnitude plot is just the singular value plot of a SISO transfer function.

### 3.3 Bound estimation model and algorithm of FTE in symmetrical plane

PBN implementation in the Next Generation

ATM system can bring more accuracy, but the safety of life-critical aviation is always the primary goal to fulfill. For safety, we need to be conservative enough. Thus, we consider the worst case to define the FTE bound.

If  $T(s)$  is stable, based on Eq. (34), the following equation holds

$$E\{y^2\} = \frac{1}{2\pi} \int_{-\infty}^{\infty} \sigma^2(\Phi_{uu}^{1/2}(\omega)T(j\omega))d\omega = \frac{1}{2\pi} \int_{-\infty}^{\infty} \sigma^2(T(j\omega))\Phi_{uu}(\omega)d\omega \quad (35a)$$

$$E\{y^2\} \leq \frac{1}{2\pi} \left[ \sup_{\omega \in (-\infty, +\infty)} \{\sigma[T(s)]\} \right]^2 \int_{-\infty}^{+\infty} \Phi_{uu}(\omega)d\omega \quad (35b)$$

$$E\{y^2\} \approx \frac{1}{2\pi} \left[ \sup_{\omega \in B_d} \{\sigma[T(s)]\} \right]^2 \int_{\omega \in B_d} \Phi_{uu}(\omega)d\omega \quad (35c)$$

where  $B_d$  is the frequency range, within which the power spectral density of dominant disturbance signal concentrates. Generally,  $B_d$  should be 2—3 times broader than band width in order to be conservative enough. The band width of  $\Phi_{uu}(\omega)$  is defined as the frequency range that  $\Phi_{uu}(\omega)$  drops down from its peak value  $\sup_{\omega \in (-\infty, +\infty)} [\Phi_{uu}(\omega)]$  to  $0.707 \sup_{\omega \in (-\infty, +\infty)} [\Phi_{uu}(\omega)]$ .

Note that  $T(s)$  in Eq. (35) stands for a specific SISO transfer function of concerned input signal and output signal pair. In such a case, the highest and the lowest gain directions of MIMO system are unified into the same one, while the highest gain direction (corresponding to the maximum singular value) and the lowest gain direction (corresponding to the minimum singular value) are used to account for the directions of the maximum major semi-axis and the minimum minor semi-axis of image hyperellipsoid in an MIMO case.

Based on the aforementioned work, calculating procedure of FTE upper bound is outlined briefly as:

(1) Plot the power spectral density of lateral Dryden turbulence fluctuation.

(2) Determine the band width of power spectral density, then define  $B_d$  as 2—3 times of the bandwidth.

(3) Based on the transfer matrix of compensated closed-loop system, acquire SISO transfer functions with white Gaussian noise as input and

$h, v$  as output.

(4) Plot the Bode magnitude plot of each SISO transfer functions. The frequency range of  $B_d$  should be included.

(5) Determine the maximum values of the Bode magnitude curve on the frequency range of  $B_d$ .

(6) If the wind speed at 20 ft (6.156 m) is obtained, the turbulence intensity category can be determined. Then calculate the upper bound of the longitudinal FTE variance and vertical FTE variance with Eq. (35c).

(7) If the wind speed at 20 ft (6.156 m) is not obtained, the upper bounds of longitudinal FTE variance and vertical FTE variance can be calculated with Eq. (35c) for different turbulence intensity (light, moderate and severe).

(8) Calculate the mean value of the three variance values of different turbulence intensity according to different probability<sup>[9]</sup>.

### 3.4 Calculation of FTE in symmetrical plane

As shown in Table 1, the upper bound values of standard deviation of FTE in symmetrical plane are calculated according to Eq. (35c) and the calculating procedure. Note that we exemplify here the most general case that the turbulence intensity is not determined. If we can obtain the accurate required meteorological parameters, i. e. wind velocity at 20 ft (6.156 m), then the turbulence intensity is determined and only one specific turbulence intensity needs to be considered.

Make  $B_d$  equal  $[-5.5]$  in order to be conservative enough to include the frequency region where the power spectral densities of both longitudinal and vertical turbulence fluctuation dominantly concentrate. Also note that the functions plotted in Fig. 4 are even.

**Table 1 Upper bound of standard deviation of FTE in symmetrical plane and probability values for three turbulences**

Turbulence Intensity	Light	Moderate	Severe
Probability	$9.1800 \times 10^{-18}$	$8.2000 \times 10^{-21}$	$1.3615 \times 10^{-5}$
$\sigma_{\max}(h)/\text{ft}$	19.671	39.341	59.012
$\sigma_{\max}(v)/\text{ft}$	14.505	29.010	43.516

The expectation of standard deviation of FTE during final approach is obtained by

$$E[\sigma_{\text{FTE}}(h)] = P_1 \times \sigma_1(h) + P_m \times \sigma_m(h) + P_s \times \sigma_s(h) = 21.285 \quad (36)$$

$$E[\sigma_{\text{FTE}}(v)] = P_1 \times \sigma_1(v) + P_m \times \sigma_m(v) + P_s \times \sigma_s(v) = 15.695 \quad (37)$$

where  $P_1$ ,  $P_m$ ,  $P_s$  are the probability values corresponding to light, moderate and severe turbulence intensity respectively, as shown in Table 1.

## 4 SIMULATION AND DISCUSSION

### 4.1 Simulation configuration and results

The forming filter of Dryden turbulence is integrated into the optimal compensated ARIC model, thus the integrated system is driven by zero mean white Gaussian noise. In the integrated system, the state variables of the state-space realization of the forming filter is added into that of the state equations of the closed-loop compensated control system.

The Dryden turbulence fluctuation is generated with the following parameters; Flight altitude is 900 ft (277.02 m);  $W_{20}$  is 15 knots for typical light turbulence; Air speed  $V$  is 229.67 ft/s (about 70.69 m/s) for typical approach velocity of transport jets. For the practical estimation of FTE in symmetrical plane, the cases of moderate as well as severe turbulence intensity are also necessary. Correspondingly,  $W_{20}$  is 30 knots and 45 knots respectively.

**Table 2 Unbiased estimation of standard deviation of FTE in symmetrical plane for three turbulences**

Turbulence intensity	Light	Moderate	Severe
$\sigma_{\max}(h)/\text{ft}$	12.016	29.745	43.870
$\sigma_{\max}(v)/\text{ft}$	11.457	20.014	34.146

To validate the theoretical algorithm, Monte-Carlo simulation is used. The simulation operates 50 times for each kind of turbulence intensity (150 runs in total), each run lasts for 10 s. Then the mean values of numerical characteristics of 50 runs for different turbulence intensities are calculated (listed in Table 2) to validate

those calculated with the theoretical model.

The sample population has 100 points sampled at 0.1 s time increment from each run. The standard deviation is strongly consistent estimation with 95% confidence level and performed with some numerical statistical package, e. g. Matlab. Note that the upper bound is comparatively larger than the simulated value and calculated based on the worst case. Furthermore, the magnitude of each run is within the range bounded by  $3\sigma_{\max}$  (i. e. abide by the 3-sigma principle) and centered with mean value. This can be observed from Fig. 5.

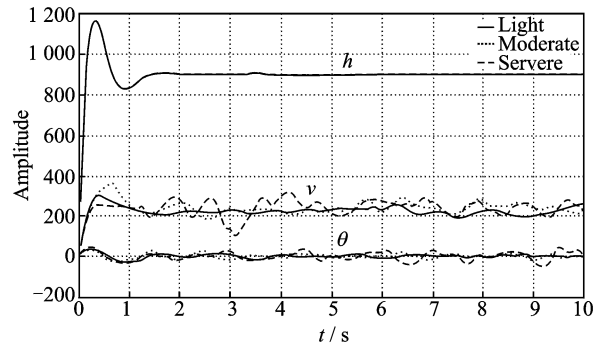


**Fig. 5** Time domain response of light Dryden turbulence disturbed longitudinal automatic control model

Fig. 5 shows the simulation results of the time domain transient response of the longitudinal automatic control model, which is disturbed by Dryden turbulence with light (moderate or severe) intensity. It is observed from Fig. 5 that the magnitude of variance of altitude deviation is quite small compared with that of pitch angle and forward air speed. It follows that the vertical channel turbulence disturbance is mainly absorbed by the short term kinematics. Thus the altitude, which is a variable of the long term kinematics, is able to maintain at the commanded reference value. It can also be noted that the magnitude of standard deviation of FTE escalates with stronger turbulence intensity.

### 4.2 Discussion

One of the most important requirements in life-critical aviation industry is safety, and with

its predominant priority the worst case is always studied and has the fundamental effect on the establishment of regulations. Consistently, the analysis and the anticipation of FTE in symmetrical plane are conducted with this principle. The results visualized in Fig. 5 are three realizations with variant turbulence intensity of the FTE stochastic process using the aforementioned configurations of automatic flight control model and environmental atmosphere turbulence model. However, the estimated FTE standard deviation value using the bound estimation model would not necessarily equals any certain simulated result, in which the algorithm considers the maximum possible FTE variance in symmetrical plane within the universal set of all realizations. As such, we believe the proposed approach and derived algorithm are viable and sound.

It is almost impossible to acquire the measured data of FTE for the identical aircraft type used in this paper, partially due to the confidentiality of AFCS parameters and other data. Also it is because that the aircraft type is not mentioned in the original reference. However, the lateral FTE of Boeing737 during final approach is specified in Ref. [10].

The concept of singular value plot is related to an MIMO system. If the system is a SISO transfer function, the singular value plot is identical with its magnitude Bode plot. However, we use analysis method based on singular value rather than that of Bode plot because this can remain consistency with the analysis and modeling of lateral FTE, which is out of the scope of this paper. In the case of lateral FTE, the lateral displacement from desired track is the dominant variance compared with that of other signals in output vector. Therefore the vector gain approach is preferred when analyzing lateral FTE. Besides, the vector gain approach is mainly based on the MIMO singular value analysis method.

Also note that the extreme value of Bode magnitude plot of a SISO transfer function is in-

deed its  $H_\infty$  norm, but what is useful for the bound estimation algorithm is the extreme value with a limited frequency range where the power spectral density of turbulence disturbance mainly focuses.

## 5 CONCLUSIONS

(1) The main contributor of FTE in symmetrical plane of AFCS engaged aircraft is environmental turbulence, and FTE increases with escalating environmental turbulence intensity.

(2) The error estimation mapping function of FTE in symmetrical plane is proposed based on the singular value theory.

(3) The bound estimation algorithm of FTE in symmetrical plane is proposed based on SISO transfer function gains and power spectral density of input driving signal.

(4) The real-data simulation result justifies the proposed model and the singular value approach in analysis of variance propagation.

(5) The bound estimation model of FTE in symmetrical plane proposed in this paper is utilized for flight technical error estimation in PBN.

### References:

- [1] DOC 9613 AN/937. Performance based navigation (PBN) manual montreal; international civil aviation organization [M]. 3rd Edition. Montreal; ICAO, 2008.
- [2] Anderson M R. Flight technical error model for non-stationary random turbulence[C]//AIAA Guidance, Navigation, and Control Conference and Exhibit Montreal. Canada; AIAA, 2001; 1-9.
- [3] Benjamin P S, Levy S, Greenhaw R. Analysis of flight technical error on straight, final approach segments [C]//59th Annual Meeting Proceedings of ION. Albuquerque, New Mexico; IEEE, 2003;456-467.
- [4] Hall T, Soares M. Analysis of localizer and glide slope flight technical error[C]//27th Digital Avionics Systems Conference. Saint Paul, Minnesota, USA; IEEE/AIAA, 2008;2.D. 2-1-2.D. 2-9.
- [5] Williams D M, Consiglio M C, Murdoch J L, et al. Flight technical error analysis of the SATS higher volume operations simulation and flight experiments

- [C]//24th Digital Avionics Systems Conference. 2005; 3. B. 1-1-13. B. 1-12.
- [6] Zhao Hongsheng, Xu Xiaohao, Zhang Jun, et al. Lateral flight technical error estimation model for performance based navigation[J]. Chinese Journal of Aeronautics, 2011, 24(3): 329-336.
- [7] Hung Y S, Macfarlane A G J. Multivariable feedback: a quasi-classical approach, lecture notes in control and information sciences [M]. Berlin: Springer-Verlag, 1982.
- [8] Military Specifications MIL-8785C[S]. USA, 1980.
- [9] Beal T R. Digital simulation of atmospheric turbulence for dryden and von karman models[J]. Journal of Guidance, Control, and Dynamics, 1993, 16: 132-138.
- [10] Shomber H R. RNP Capability of FMC Equipped 737 [M]. Generation 3. USA: Boeing Company, 2003.

## 性能基导航中对称面内飞行技术误差模型

赵鸿盛<sup>1</sup> 徐肖豪<sup>2</sup> 张 军<sup>1</sup> 朱衍波<sup>1</sup> 杨传森<sup>3</sup>

(1. 北京航空航天大学电子信息工程学院, 北京, 100191, 中国;

2. 中国民航大学空中交通管理学院, 天津, 300300, 中国;

3. 南京航空航天大学民航学院, 南京, 210016, 中国)

**摘要:** 飞行技术误差(FTE)与导航系统误差(NSE)是性能基导航(PBN)中总系统误差(TSE)的主要组成部分。性能基导航的实施需要对总系统误差进行航前预测以及航行中的短期动态预测。当飞行技术误差预测值与导航系统误差预测值的和大于PBN 导航的规定值时,将无法运行PBN 导航。因此,对于总系统误差的两个主要误差分量需要精确建模和透彻分析。采用LQG/LTR 方法针对ARIC 模型设计了多输入多输出纵向飞行控制系统,分析了在湍流扰动下进近飞行器对称面内的飞行技术误差。基于奇异值理论提出了对称面内飞行技术误差的映射函数以及边界估计模型。模型是基于对对称

面内飞行技术误差成型机理的分析提出的,提供了一种基于成型机理的分析和估计方法,从而避免了昂贵试飞和单纯的数据拟合。基于真实数据的仿真验证了对称面内飞行技术误差的理论分析。研究同时揭示了当自动飞行控制系统(AFCS)接通时性能基导航中对称面内飞行技术误差部分由湍流扰动引致,且随湍流强度的增强而增大。

**关键词:** 飞行技术误差;性能基导航;LQG/LTR;空中交通管理;Kalman 滤波

**中图分类号:** V355

(Executive editor: Zhang Huangqun)